Check for updates

An overview of the optically detected magnetic-state-selected cesium beam clock

Sifei Chen[1], Chang Liu[2], Lifeng Fan[1], Chen Liu[1], Yuanhao Li[1], Shaohang Xu[1], Chaojie Li[1] and Yanhui Wang[1]*

[1]Institute of Quantum Electronics, School of Electronics, Peking University, Beijing, China, [2]Chengdu Synchronization Technology Ltd., Chengdu, China

Among all kinds of compact cesium beam clocks, the optically detected magnetic-state-selected cesium beam clock (OMCC) combines the advantages of the magnetic state selecting scheme and fluorescence detecting method. This paper presents an overview of the OMCC. Technical issues, noise sources, frequency shifts and improvements of OMCC are reviewed. Finally, the frequency stability of five OMCC is given, which is better than the stability of the high-performance version of Microsemi 5071A.

1 Introduction

Nowadays, quantum physics has a wide range of applications, such as quantum sensors, quantum computation and quantum cryptography [1–5]. Among these applications, the atomic clock is one of the most developed precision instruments with a history of nearly 70 years [6–8]. Various atomic clocks with corresponding applications have emerged. For instance, chip-scale atomic clocks based on the coherent population trapping effect are used in communication and navigation systems [9–11], and room-sized optical lattice clocks can be used to explore the gravitational redshift effect and dark matter [12, 13]. The value of atomic clocks has already penetrated all aspects of human life. Among all kinds of atomic clocks, compact cesium beam clock plays an important role in time-keeping, telecommunication systems and navigation systems for its structural simplicity, promising long-term stability and accuracy [14].

According to the different working principles, cesium beam clocks can be divided into three categories including the magnetic state selecting cesium beam clock, the optically pumped cesium beam clock and the optically detected magnetic-state-selected cesium beam clock (OMCC). Based on the Stern-Garlach experiment, traditional cesium beam clocks use inhomogeneous magnetic fields to deflect the atomic beam, thereby realizing state preparation and state detection [15]. The second magnet, combined with the

hot-wire, the mass spectrometer and the electron multiplier, is used to convert the atomic state information into electric signal. The state-selecting magnet is velocity-selective. Therefore, atoms usually have a narrower velocity distribution, resulting in a narrower Ramsey linewidth [16, 17]. In addition, the system is simpler compared to the other two schemes, which makes it less sensitive to the environment condition. However, careful design of the beam optics is required, including the magnetic field intensity, the position of the cesium oven, etc. The short-term stability is often limited by the atomic shot noise due to the low density of the atomic beam [6]. Besides, technical issues are often the limiting factor for the lifetime of the electron multiplier. At present, the most widely used commercial cesium beam clock, Microsemi 5071A, is based on this scheme and has negligible frequency variation with environmental changes [18]. The fractional frequency stability of the high-performance version reaches $8.5 \times 10^{-12}\tau^{-1/2}$. Another product Cs3000C developed by Lanzhou Institute of Physics has the same stability level with 5071A [19].

Around 1980, the optical pumping technique was developed and applied to cesium beam clocks combined with the laser induced fluorescence method [20–22]. Compared with the magnetically-selected cesium atomic clock, the optically pumped cesium clock greatly improves the atom utilization efficiency and achieves a high signal-to-noise ratio. The beam optics system is simple, but the pumping light and detecting light inevitably introduce light shift into the system, which deteriorate the long-term stability. Typical compact optically pumped cesium clocks include OSA-3350 by Oscilloquartz, TA1000 by Chengdu Space on Electronics [23], and optical pumped clocks developed by Peking University [24, 25].

To combine both the advantages of the two schemes and avoid the technical issues concerning the lifetime of the electron multiplier, we proposed the magnetic-state-selecting and optical detecting scheme in 2009. After preliminary design and preparation, the first prototype was built in 2015 [26]. The short-term stability was $1.0 \times 10^{-11}\tau^{-1/2}$, which is comparable to the standard version of 5071A. To improve the long-term stability, the microwave power and C-field were stabilized, and the 5-days stability reached 2.7×10^{-14} [27]. Having optimized the stabilization scheme, the design of the cesium beam tube and the laser stabilization method, we improved the frequency stability to $4.1 \times 10^{-12}\tau^{-1/2}$, which is better than the high-performance version of 5071A [28].

This paper is an overview of the cesium beam clocks based on the magnetic-state-selecting and optical detecting scheme. In Section 2 we introduce the structure and working principle of OMCC. Section 3 focuses on its short-term and long-term stability. Optimizations concerning both the short-term and long-term stability are also summarized.
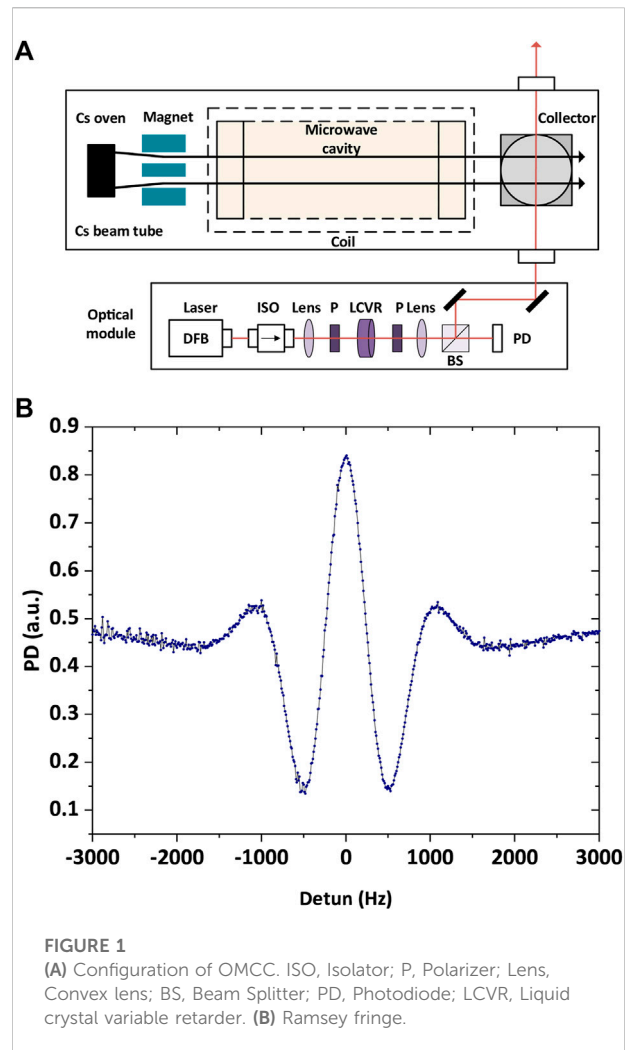

FIGURE 1
(A) Configuration of OMCC. ISO, Isolator; P, Polarizer; Lens, Convex lens; BS, Beam Splitter; PD, Photodiode; LCVR, Liquid crystal variable retarder. **(B)** Ramsey fringe.

2 Principles

The schematic of OMCC is depicted in Figure 1A. As introduced previously, OMCC is a compact cesium beam atomic clock based on the magnetic-state-selecting and optical-detecting scheme. Great care has been taken in the design of the cesium beam tube, the optical setup and the servo electronics for promising frequency stability. Here we briefly describe the outline of the system.

2.1 Cesium beam tube

The cesium beam tube adopts the double-beam structure. Compared with the single beam structure, its advantage is that it has a larger beam intensity at the same oven temperature. The cesium atoms are heated and ejected through a folded collimator [29]. We use a magnet based on the two-wire configuration to select the state of atoms in each beam [17]. Atoms in state $|F = 3\rangle$

are selected. The maximum gradient in the state selection direction is about −0.48 T/mm.

The cesium atoms in state $|F = 3\rangle$ enter the U-shaped microwave cavity and interact with the microwave field. The resonant frequency of the cavity is designed to be 9.192 GHz. The length of the single-action region is 1 cm. The distance between the two arms is 16 cm. Oxygen-free copper with high conductivity is used as the material to minimize the influence of the cavity phase difference. After tuning, the loaded quality factor of the microwave cavity is about 300–400. A static magnetic field is induced by the coils around the cavity to distinguish the transition state $|F = 3, m_F = 0\rangle - |F = 4, m_F = 0\rangle$ from others to avoid the first-order Zeeman shift. The orientation of the so-called C-field is the same as the state-selecting magnetic field for the same quantization axis for atoms to avoid Majorana transition. Three layers of magnetic shielding are applied to reduces the effect of ambient magnetic fields.

In order to improve the detection signal-to-noise ratio, a laser resonant with the cyclic transition line of the cesium D_2 line, $|F = 4 - F' = 5\rangle$, is used to realize the fluorescence detection of the $|F = 4\rangle$ atoms. Each atom in the light field can emit an average of 200–300 fluorescent photons, which is superior to other transition lines. Two spherical mirrors with different focal length are used as a fluorescence collector to converge the fluorescence onto the photodiode. The overall collection efficiency is estimated to be about 30%. Figure 1B shows the typical Ramsey fringe of OMCC. Due to the velocity-selective effect of the state-selecting magnet, the most probable velocity of the atomic beam is slower, which results in the linewidth of the OMCC being 1.5 to 2 times narrower than that of optical pumped compact cesium clocks [28].

2.2 Optical setup

The detecting light is generated by a distributed-feedback (DFB) laser (Eagleyard EYP-DFB-0852). The typical linewidth is 2 MHz which is narrower than the natural linewidth of the transition line. The optical isolator is magnetically shielded to reduce the magnetic flux leakage to the cesium beam tube. For the OMCC to operate continuously and stably, the laser frequency needs to be stabilized. Previously, the laser frequency was stabilized to the saturated absorption spectroscopy. There are some disadvantages practically. First, due to the multi-peak nature of the saturated absorption spectrum, the laser frequency is likely to be mis-locked to other peaks. The amplitude of the cyclic transition line is small compare to crossover lines in saturated absorption spectroscopy. Second, the saturated absorption spectrum is based on the atomic vapor cell, which is greatly affected by the motion of atoms, that is, by the ambient temperature. Under the saturable absorption spectrum frequency stabilization scheme of optically pumped cesium atomic clocks in literature, the laser frequency stability

begins to deteriorate when the average time exceeds 100 s [30]. In addition, the saturated absorption spectrum system induces the structural complexity of the optical system, which is unfavorable to the long-term stability of OMCC.

Instead, we adopt the fluorescent spectroscopy to stabilize the laser frequency. Laser frequency is kept resonant with the atomic beam, and the mis-locking problem is avoided. The laser current is modulated, and the fluorescent signal is demodulated with the same sinusoidal wave in phase to generate the error signal. The error signal is processed by the PID module and fed back to the laser current. The loop bandwidth is about 200 Hz.

Practically, we found that there is a long-term drift in the laser power. The Allan deviation of the laser power is 4.5×10^{-3} at 10^5 s. After thorough investigation, we found that the drift results from the temperature drift of resistors in the circuit. A liquid crystal variable retarder (LCVR, Thorlabs, LCC-1111B) is used to tune the polarization of the light and stabilize the laser power. With this method, the laser power stability is increased to 3×10^{-6} at 10^5 s [31].

2.3 Servo

In order to improve the continuous running time and long-term frequency stability of OMCC, a digital servo system based on Field Programmable Gate Array (FPGA) is implemented [32]. The microwave frequency is modulated with a square wave at 10^2 Hz for the maximum error signal slope.

Conventionally, the power of the microwave field is stabilized to the response of microwave transition line to the microwave amplitude. The FPGA outputs a square wave voltage through the DAC to the voltage-controlled attenuator, forming a slow square wave modulation on the microwave power. The error signal is generated by demodulating the fluorescent signal. However, according to Ref. [17], the amplitude of the microwave field for which the error signal reaches the maximum value is not identical to that which maximize the transition probability. Thus, we demodulate the microwave frequency error signal instead to stabilize the power of the microwave field [28]. The method also minimizes the cavity pulling shift.

The strength of the C-field is stabilized *via* the adjacent transition $|F = 3, m_F = 1\rangle$ to $|F = 4, m_F = 1\rangle$ for its resonant frequency is proportional to the C-field. The FPGA changes the frequency to the neighboring transition every 100 s. The error signal is then used to lock the C-field.

3 Frequency stability

The frequency stability of an OMCC is affected by both the noise sources and frequency shift. Here we only introduce a few factors that have the greatest impact on the frequency stability, including atomic shot noise and laser frequency noise affecting

the short-term stability, and the light shift which limiting the long-term stability.

3.1 Noise sources

The short-term frequency stability of passive cesium atomic clocks mainly depends on the Ramsey spectral line signal-to-noise ratio (SNR) and spectral linewidth. The linewidth is determined by the beam optics design, as discussed in Section 2.1. SNR refers to the ratio of the amplitude of the Ramsey fringe and the amplitude of the noise at the modulation frequency. Noise sources are considered uncorrelated, thus the corresponding power spectrum density (PSD) can be summed directly. Reference [28] shows the detailed analysis over the SNR of the OMCC.

The main noise sources of an OMCC including the atomic shot noise, laser frequency noise, photon shot noise, detecting noise, and noise in the electronics. Firstly, the atomic shot noise comes from the particle nature of the atomic beam. Atoms reach the detection zone randomly, which arousing the shot noise in the fluorescence signal [33]. The SNR corresponding to the atomic shot noise is proportional to $I_e/(I_r + \frac{1}{2}I_e)^{1/2}$, where I_e is the amplitude of the microwave spectrum, and I_r is the fluorescent signal contributed by unwanted atoms in the detected beam because of the unideal state selection [28]. The SNR corresponding to the shot noise is proportional to the square root of the atomic flux when the ratio I_r/I_e is a constant. Therefore, to increase the SNR, one possible way is to raise the oven temperature for the higher atomic flux. Since the beam optics is determined by the state-selecting magnet and mechanical structure, the velocity distribution and state selecting efficiency are not affected when raising the temperature.

Another noise source is the laser frequency noise. The fluctuation of the laser frequency results in the fluctuation of the detection signal. The PSD of the detection signal corresponding to the laser frequency noise is given in Ref. [34]. The SNR, correspondingly, is proportional to $I_e/(I_r + \frac{1}{2}I_e)$. The coefficient shows that laser frequency noise is not relevant with the total beam flux, but only relevant with the state selecting efficiency. Thus, simply raise the oven temperature does not influence the SNR corresponding to the laser frequency noise. This part of SNR is the upper limit for the SNR of a cesium beam tube. One possible solution is to use the laser with narrower linewidth. Another method is to appropriately increase the laser power to produce saturation broadening of the fluorescence spectrum.

There are other noise sources in an OMCC. The photon shot noise originates from the randomness of atomic radiation. The detecting noise comes from the imperfection of the collecting efficiency of the fluorescence
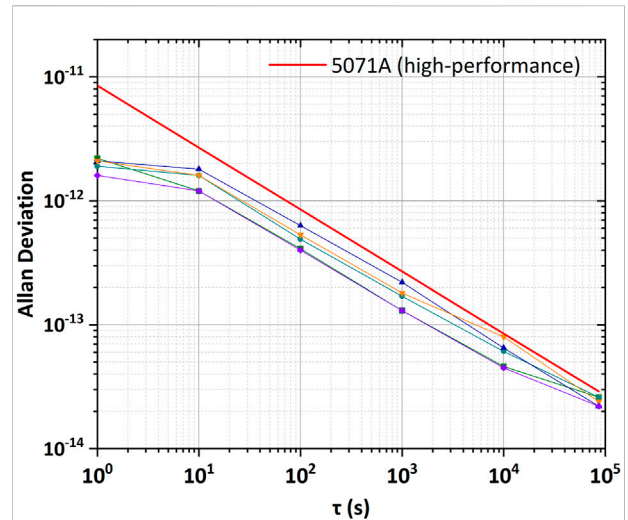

FIGURE 2
Frequency stability test result of five OMCC in comparison with the high-performance version of 5071A.

collector. There are also noise sources in the circuit, including the dark current of the photodiode, the thermal noise of resistors, etc. The PSD corresponding to these noise sources is often negligible to that of the atomic shot noise and laser frequency noise [28].

3.2 Long-term stability

The long-term stability of the OMCC is affected by several frequency shifts. The largest one is the quadratic Zeeman shift. The energy shift of cesium atoms interacting with static magnetic field can be calculated with Breit-Rabi formula. For the clock transition states $|F = 3, m_F = 0\rangle - |F = 4, m_F = 0\rangle$, the transition frequency can be written as

$$\nu = \nu_0 + 427.44H_0^2$$

where ν_0 is the unperturbed hyperfine transition frequency of 9192631770 Hz, and the unit of the strength of the magnetic field H_0 is Oersted. The frequency difference between 0–0 line and 1–1 line ($|F = 3, m_F = 1\rangle - |F = 4, m_F = 1\rangle$) is used to stabilize the C-field current, therefore reducing the long-term frequency fluctuation due to the drift of the ambient magnetic field.

One another frequency shift is the light shift. In OMCC, both the stray light and fluorescence inevitably diffuse into the microwave cavity and shift the central frequency. The light shift changes with the deformation of the optical path and the drift of the laser power. To reduce the light shift coefficient, we apply the laser power stabilization loop, as discussed in Section 2.3. The optical module is designed to be as compact as possible to reduce the long-term deformation

effect. Moreover, we find that it is possible to introduce a detuned laser into the detection light [35, 36]. With properly chosen frequency and intensity, the method can sufficiently suppress the light shift coefficient by more than an order of magnitude.

3.3 Result

The frequency stability test result of five OMCC at National Institute of Metrology in China is plotted in Figure 2. The frequency reference is an active hydrogen maser and the measure time is over 15 days. With carefully designed loop gain, the short-term stability at $\tau < 10$ s is determined by the stability of the crystal oscillator. From 10 to 10^5 s, the slope of the Allan deviation curve is $-1/2$, indicating that the dominating noise is white frequency noise. The result shows promising frequency stability and good consistency of OMCC.

4 Conclusion

In this paper, we review the basic principles of optically detected magnetic-state-selected cesium atomic clocks and some improvements we have made. In comparison with the traditional magnetic state selecting atomic clock and optical pumped atomic clock, OMCC has unique advantages in systematic simplicity and frequency stability. After 13 years of development, we can now achieve the better frequency stability than the high-performance version of 5071A, which proves that the scheme is quite promising. For better performance, we are now focusing on cesium beam tube design, accuracy evaluation and improvements on the environmental adaptability.

Author contributions

CaL, YW contributed to the conception of the reviewed scheme. CaL, LF, CeL, and CLi contributed to experimental setup. SC contributed to data analysis and data visualization. SC wrote the manuscript. YL and SX contributed to manuscript preparation.

Funding

Conflict of interest

Author CaL is employed by Chengdu Synchronization technology Ltd.

The remaining authors declare that the research was conducted in the absence of any commercial or financial relationships that could be construed as a potential conflict of interest.

Publisher's note

All claims expressed in this article are solely those of the authors and do not necessarily represent those of their affiliated organizations, or those of the publisher, the editors and the reviewers. Any product that may be evaluated in this article, or claim that may be made by its manufacturer, is not guaranteed or endorsed by the publisher.

References

1. Degen CL, Reinhard F, Cappellaro P. Quantum sensing. *Rev Mod Phys* (2017) 89(3):035002. doi:10.1103/RevModPhys.89.035002

2. Kitching J, Knappe S, Donley EA. Atomic sensors - a review. *IEEE Sens J* (2011) 11(9):1749–58. doi:10.1109/Jsen.2011.2157679

3. Montanaro A. Quantum algorithms: An overview. *Npj Quan Inf* (2016) 2: 15023. doi:10.1038/npjqi.2015.23

4. Ma HY, He ZX, Xu PG, Dong YM, Fan XK. A quantum richardson-lucy image restoration algorithm based on controlled rotation operation and Hamiltonian evolution. *Quan Inf Process* (2020) 19(8):237. doi:10.1007/s11128-020-02723-4

5. Lo HK, Curty M, Tamaki K. Secure quantum key distribution. *Nat Photon* (2014) 8(8):595–604. doi:10.1038/Nphoton.2014.149

6. Cutler LS. Fifty years of commercial caesium clocks. *Metrologia* (2005) 42(3): S90–S9. doi:10.1088/0026-1394/42/3/s10

7. Essen L, Parry JVL. Caesium resonator. *Nature* (1955) 176(4476):281–2. doi:10. 1098/rsta.1957.0010

8. Vanier J, Audoin C. The classical caesium beam frequency standard: Fifty years later. *Metrologia* (2005) 42(3):S31–S42. doi:10.1088/0026-1394/42/3/s05

9. Freeman SE, Emokpae LE, Edelmann GF. High-frequency, highly directional short-range underwater acoustic communications. In: Oceans 2015 - MTS/IEEE Washington; 19-22 October 2015; Washington, DC, USA. IEEE (2015). p. 1–4.

10. Rybak MM, Axelrad P, Seubert J, Ely T. Chip scale atomic clock-driven one-way radiometric tracking for low-earth-orbit cubesat navigation. *J Spacecr Rockets* (2021) 58(1):200–9. doi:10.2514/1.A34684

11. Zhan LW, Liu Y, Yao WX, Zhao JC, Liu YL. Utilization of chip-scale atomic clock for synchrophasor measurements. *IEEE Trans Power Deliv* (2016) 31(5): 2299–300. doi:10.1109/Tpwrd.2016.2521318

12. Bothwell T, Kennedy CJ, Aeppli A, Kedar D, Robinson JM, Oelker E, et al. Resolving the gravitational redshift across a millimetre-scale atomic sample. *Nature* (2022) 602(7897):420–4. doi:10.1038/s41586-021-04349-7

13. Kennedy CJ, Oelker E, Robinson JM, Bothwell T, Kedar D, Milner WR, et al. Precision metrology meets cosmology: Improved constraints on ultralight dark matter from atom-cavity frequency comparisons. *Phys Rev Lett* (2020) 125(20): 201302. doi:10.1103/PhysRevLett.125.201302

14. Jaduszliwer B, Camparo J. Past, present and future of atomic clocks for GNSS. *Gps Solut* (2021) 25(1):27. doi:10.1007/s10291-020-01059-x

15. Marlow BLS, Scherer DR. A review of commercial and emerging atomic frequency standards. *IEEE Trans Ultrason Ferroelectr Freq Control* (2021) 68(6): 2007–22. doi:10.1109/TUFFC.2021.3049713

16. Becker G. Recent progress in primary Cs beam frequency standards at the PTB. *IEEE Trans Instrum Meas* (1976) 25(4):458–65. doi:10.1109/Tim.1976. 6312264

17. Vanier J, Audoin C. *The quantum physics of atomic frequency standards*. Bristol and Philadelphia: Adam Hilger (1989).

18. Kalliomaki K, Mansten T, Mannermaa J. Short and long term stability of HP Cs standards including environmental effects. In: 18th European Frequency and Time Forum (EFTF 2004); 05-07 April 2004; Guildford: IET (2004). p. 409–10.

19. Chen J, Wang J, Ma P, Guo L, Tu J, Yang W, et al. Test of magnetic-selected cesium atomic clock LIP Cs3000C. *J Time Frequency* (2018) 41(3):190–3. doi:10.13875/j.issn.1674-0637.2018-03-01.90-04

20. Arditi M, Hirano I, Tougne P. Optical pumping of a caesium beam and detection of the 0-0 'clock' transition. *J Phys D Appl Phys* (1978) 11(18):2465–75. doi:10.1088/0022-3727/11/18/005

21. Lewis L, Feldman M. Optical pumping by lasers in atomic frequency standards. In: Thirty Fifth Annual Frequency Control Symposium; 27-29 May 1981; Philadelphia, PA, USA. IEEE (1981). p. 612–24.

22. de Clercq E, de Labachellerie M, Avila G, Cerez P, Tetu M. Laser diode optically pumped caesium beam. *J Phys France* (1984) 45(2):239–47. doi:10.1051/jphys:01984004502023900

23. Zhao X, Chen H, Yang L, Wei Q, Li D, Li Y. Stabilizing the optical frequency by laser-induced fluorescence in optically pumped Cs beam frequency standard. *J Astronautic Metrology Meas* (2020) 40(1):17–22. doi:10.12060/j.issn.1000-7202.2020.01.03

24. Xie W, Wang Q, He X, Chen N, Xiong Z, Fang S, et al. Frequency instability of a miniature optically pumped cesium-beam atomic frequency standard. *Rev Sci Instrum* (2020) 91(7):074705. doi:10.1063/5.0001749

25. He X, Fang S, Yuan Z, Xie W, Chen N, Xiong Z, et al. Compact optically pumped cesium beam atomic clock with a 5-day frequency stability of $7{\times}10^{-15}$. *Appl Opt* (2021) 60(34):10761–5. doi:10.1364/AO.443812

26. Liu C, Zhou S, Wang Y. Noise investigation on optical detection in a cesium beam clock with magnetic state selection. In: 2015 Joint Conference of the IEEE International Frequency Control Symposium & the European Frequency and Time Forum (IFCS/EFTF); 12-16 April 2015; Denver, CO, USA. IEEE (2015). p. 483–6.

27. Liu C, Wang S, Chen Z, Wang Y, Jia J, Sun Y, et al. A caesium atomic beam microwave clock detected by distributed feedback laser diodes. In: 2017 Joint

Conference of the European Frequency and Time Forum and IEEE International Frequency Control Symposium (EFTF/IFCS); 09-13 July 2017; Besancon, France. IEEE (2017). p. 282–4.

28. Liu C, Chen S, Chen Z, Li L, Xu S, Li Y, et al. Improving the short-term frequency stability of a magnetic-state-selected cesium beam clock with optical detection. *Rev Sci Instrum* (2021) 92(7):073302. doi:10.1063/5.0046575

29. Jones RH, Olander DR, Kruger VR. Molecular-beam sources fabricated from multichannel arrays. I. Angular distributions and peaking factors. *J Appl Phys* (1969) 40(11):4641–9. doi:10.1063/1.1657245

30. Wang Q, Duan J, Qi X-H, Zhang Y, Chen X-Z. Improvement of laser frequency stabilization for the optical pumping cesium beam standard. *Chin Phys Lett* (2015) 32(5):054206. doi:10.1088/0256-307x/32/5/054206

31. Chen Z, Liu C, Wang S, Wang Y. A method on laser power stabilization in optical detection cesium atomic clock. In: China Satellite Navigation Conference (CSNC) 2018 proceedings, Harbin, China, 23 May, 2018. Springer (2018). p. 607–14.

32. Liu C, Wang S, Chen Z, Wang Y, Hou S. Optical detection in magnetic state-selection Cs beam tubes for transportable Cs beam clocks. *Meas Sci Technol* (2019) 30(7):075004. doi:10.1088/1361-6501/ab11af

33. Dimarcq N, Audoin C. Detection of atoms in a beam - filtering of the atomic shot-noise and velocity dispersion contribution. *J Phys B: Mol Opt Phys* (1995) 28(11):2083–94. doi:10.1088/0953-4075/28/11/008

34. Dimarcq N, Giordano V, Cerez P. Statistical properties of laser-induced fluorescence signals. *Appl Phys B* (1994) 59(2):135–45. doi:10.1007/Bf01081164

35. Xu S, Chen S, Liu C, Li Y, Wang J, Wang Y. A new method to suppress the Ac-Stark shift of compact cesium beam atomic clocks. In: China Satellite Navigation Conference (CSNC 2021) 2021 Proceedings, Nanchang, China, 26 May, 2021. Springer (2021). p. 17–25.

36. Xu S, Chen S, Liu C, Li Y, Wang J, Wang Y, et al. Optimization of frequency shifts in optically detected magnetic-state-selection cesium beam atomic clocks. *Europhys Lett* (2022) 136(2):23002. doi:10.1209/0295-5075/ac1bc7